Computing Systems in Engineering Vol. 2, No. 5/6, pp. 541–555, 1991
Printed in Great Britain.

0956-0521/91 $3.00 + 0.00

ADVANCES IN THE MODELING OF LAMINATED PLATES

J. N. REDDY and R. C. AVERILL
Department of Engineering Science and Mechanics, Virginia Polytechnic Institute and State University, Blacksburg, VA 24061, U.S.A.

(*Received* 10 *May* 1991)

Abstract—A review of refined two-dimensional theories and computational models of laminated composite plates is presented. The classical and various shear deformation plate theories are presented, and recent research in these areas is reviewed. A generalization of refined theories is proposed and it's special forms are discussed. Computational aspects of the displacement finite element models of the refined theories are reviewed.

1. INTRODUCTION

Composite materials are increasingly used in aerospace, underwater, and automotive structures. This is largely because many composite materials exhibit high strength-to-weight and stiffness-to-weight ratios, which make them ideally suited for use in weight-sensitive structures. The many advantages of composite materials will play an even larger role in future generations of transportation vehicles, as well as in recreational, athletic, and medical equipment, and numerous other applications. To take advantage of the full potential of composite materials, structural analysts and designers must have extremely accurate tools of analysis and design methods at their disposal.

Laminated composite structures are made up of layers of orthotropic materials that are bonded together. The layers may be of different materials and thicknesses, with the principal material directions of each layer oriented at different angles to the reference axes. By altering the material, thickness or orientation of each layer, a structural designer can tailor the strength and other properties of a laminate to the requirements of a given application.

The analysis of composite laminates is complicated because of the anisotropic structural behavior that couples in-plane deformation to out-of-plane deformation (i.e. bending–stretching coupling), complicated constituent interactions that require more in-depth understanding to formulate the constitutive, failure, and damage models, and many special requirements of composite structures that are either not present in their metallic counterparts or only characteristic of composite materials (e.g. delaminations, terminating plies, matrix cracks, fiber breakage and waviness). One of the important steps to develop accurate analysis of structures made of laminated composite materials is to select a proper structural theory (i.e. kinematics) for the problem. Of course, the choice is dictated by the specific structural problem at hand and the modes of kinematics to be studied. For example, if global response characteristics, such as the maximum deflection, fundamental frequency, or critical buckling load are needed, laminate theories that describe the laminate as an equivalent single layer can be used. If interlaminar stresses are to be determined accurately in thick laminates or delaminations and their growth to be modeled, layerwise theories must be used. Most analyses of composite laminates to date utilize single-layer theories, which are extensions of the plate theories available for isotropic plates.

The objective of this paper is to present a critical review of the single-layer laminate plate theories, present a unified third-order theory that contains lower-order theories as special cases, and describe finite element models and computational aspects of various plate theories. Recent papers by the authors[1–5] and others[6–10] form a background for the present study.

2. A REVIEW OF LAMINATE THEORIES

It is well known that the classical theory of plates introduced by Kirchhoff and extended to composite laminates[11–15] is inadequate in modeling laminated composite plates. The Kirchoff assumptions amount to treating plates to be infinitely rigid in the tranverse direction and neglecting the transverse strains. This theory underestimates deflections and overestimates natural frequencies and buckling loads. Since laminated composite materials are often very flexible in shear, and weaker in transverse shear mode, transverse shearing strains must be taken into account if an accurate representation of the behavior of the laminated plate is to be achieved.

Numerous plate theories that include transverse shear deformations are documented in the literature[16–40] (also see the references in Refs 1–3). In these theories the displacement of stress components are expanded as a linear combination of the thickness coordinate and undetermined functions of position in the reference surface to reduce the three-dimensional (3-D) elasticity problem to a two-dimensional (2-D) one. The governing equations are derived either using virtual work principles or by weighted-integrals of the 3-D stress-equilibrium equations through the thickness of the laminate—yielding an equivalent single-layer plate theory. In this study we consider plate theories based on assumed displacement expansions.

The theories based on displacement expansion can be found in the works of Basset,[16] Hildebrand *et al.*,[21] Hencky,[20] Mindlin,[22] and others.[24–32,35–37] In the displacement-based theories, the three components of the displacement vector are expanded in power series of the thickness coordinate and unknown functions. The principle of virtual displacements or the method of moments is used to derive the equations of equilibrium. In all single-layer plate theories the displacements and strains are continuous through the laminate thickness (i.e. single-valued at interfaces of layers). This leads to a discontinuous interlaminar stress field because of different elastic coefficients at layer interfaces when constitutive equations are used to compute stresses.

The most widely used displacement based theory is the *first-order shear deformation theory*. The theory is based on the displacement field

$$u_\alpha = U_\alpha + z\phi_\alpha \quad (\alpha = 1, 2)$$

$$u_3 = U_3,$$

and is known more commonly as "the Mindlin plate theory"; the original idea of such expansion can be found in earlier works by Basset,[16] Hildebrand *et al.*,[21] and Hencky.[20] The functions (U_α, U_3) denote the displacements along the three coordinate lines of a point on the reference surface, often the midsurface, and ϕ_α are the rotations of a transverse normal. The first-order shear deformation theory yields a constant value of transverse shear strain through the thickness of the plate and thus requires shear correction factors. The shear correction factors are dimensionless quantities introduced to account for the discrepancy between the constant state of shear strains in the first-order theory and the quadratic distribution of shear strains in the elasticity theory. For composite laminates, the shear correction factors, in general, depend on the constituent ply properties, lamination scheme, and type of structure (i.e. geometry and boundary conditions).[41–43] Stavsky[44] extended the first-order shear deformation theory of isotropic plates to plates laminated of isotropic layers. The work was extended to anisotropic laminates by Yang *et al.*[45] and Whitney and Pagano[46,47] studied the effect of shear deformation on bending and free vibration response of simply supported rectangular laminates according to the first-order shear deformation theory.

Second and higher-order plate theories involve higher-order expansions of the displacement field. For example, the third-order theory of Reddy[35] is based on the displacement field:

$$u_\alpha = U_\alpha + z\phi_\alpha + z^3\left[-\frac{4}{3h^2}(\phi_\alpha + U_{3,\alpha})\right](\alpha = 1, 2)$$

$$u_3 = U_3, \quad (1)$$

where $U_{3,\alpha} \equiv \partial U_3/\partial x_\alpha(\alpha = 1, 2)$. The displacement field accommodates the vanishing of transverse shear strains (and hence stresses) on the top and bottom of a laminate. The theory was extended[36] to include the von Kármán strains.

The displacement field of the type in Eq. (1) was also considered by others (e.g. Levinson,[30] Murthy,[32] and Bhimaraddi and Stevens[37]). The works of Vlasov,[39] Jemeilita,[25] Schmidt,[26] Krishna Murty,[27] and Levinson[30] were restricted to isotropic plates, and Schmidt[26] and Levinson[30] used the equilibrium equations based on the method of moments. Murthy[32] used the same approach to obtain the equilibrium equations but cast the approach in terms of the thickness-averaged displacement field. The technical note of Krishna Murty[27] suggested a general, higher-order displacement field of the type in Eq. (1). The work of Schmidt[26] also accounts for the von Kármán strains but is restricted to isotropic plates. The displacement field used by Bhimaraddi and Stevens[37] is the same as that used by Levinson and Reddy but recast in terms of different variables, which are convenient in finite element model development. Indeed, all displacement-based theories up to and including third-order theories can be obtained from a single displacement field, as shown recently by Reddy.[3] Reddy's strain-consistent third-order theory[3] is by far the most general technical theory of plates.

Librescu's theory[48] accounts for specified nonzero surface tractions on the bounding planes in the derivation of the third-order theory (also, see Ambartsumyan[12] and Jemeilita[25]). The transverse normal stress is brought into the theory by integrating the third equilibrium equation of elasticity. Jemeilita[25] also included nonzero transverse shear stresses and accounted for transverse normal stress.

Theories higher than third-order are not considered by anyone because they are cumbersome and do not result in appreciable accuracy of the solution. The third-order theory yields quadratic variation of transverse shear strains and hence does not require shear correction factors. As will be discussed later in this paper, the computational models of the theory are also very efficient.

Derivation of the equations of motion of a refined theory by the method of moments may have two disadvantages. First, the resulting equations are inconsistent with virtual work considerations and may result in non-self adjoint equations. With a judicious choice of the weight functions, one may obtain the same equilibrium equations as in the energy method. Second, the boundary conditions of the theory are not derived from the theory directly but are based on physical arguments. This aspect is the most crucial one in the higher-order theories. Reddy's theory[35] was based on the principal of virtual displacements and it yields self-adjoint equations and a unique set of boundary conditions.

Although most higher-order theories begin with the displacement field, or its special forms, the governing equations differ considerably from each other. One source of the difference is, as noted earlier, the method of deriving them: use of the method of moments or the principles of virtual work. Other sources of difference include: the choice of variables, accounting for various degrees of geometric nonlinearities, inclusion of the transverse normal stress, and satisfaction of specified (zero or non-zero) transverse shear stress conditions on the plate surfaces. Existence of solutions to Reddy's nonlinear plate theory[36] is presented by Bielski and Telega[49] (also see Refs 50–51).

Finite element analysis of the first-, second- and third-order theories can be found in the works of several authors. Finite element models of the first-order theory as applied to composite plates can be found in Refs 52–57 and references therein. Kant and his colleagues[58–61] presented finite element analysis of composite laminates based on second- and third-order theories. Engblom and Ochao[62] presented a finite element analysis of a second-order shear deformation theory. Phan and Reddy[63] and Ren and Hinton[64,65] developed displacement finite element models of Reddy's theory[35] with C^1-interpolation of the transverse deflection and C^0-interpolation of the other variables. Mixed finite element models of the Reddy's third-order theory[35,36] were developed in Refs 66–69. The third-order theory of Lo *et al.*[29] was used recently by Doong[70] to study vibration and stability of initially stressed thick plates. Most recently, Averill and Reddy reviewed shear locking in plate elements based on the first-order theory[4] and the third-order theory.[5] More discussion on shear locking is presented in Sec. 4.

3. A GENERALIZATION OF REFINED THEORIES

All technical theories up to and including third-order can be derived from the displacement field,

$$u_\alpha = U_\alpha + z\phi_\alpha + z^2\psi_\alpha + z^3\theta_\alpha \quad (\alpha = 1, 2),$$

$$u_3 = U_3 + z\phi_3 + z^2\psi_3 + z^3\theta_3. \tag{2}$$

All variables U_α, ϕ_α, ψ_α, θ_α, U_3, ϕ_3, ψ_3 and θ_3 are functions of x_α and time t. Note that the stretching of transverse normals is accounted in the displacement field (2).

The strains associated with the displacement field (2) are

$$\epsilon_{\alpha\beta} = \epsilon_{\alpha\beta}^{(0)} + z\epsilon_{\alpha\beta}^{(1)} + z^2\epsilon_{\alpha\beta}^{(2)} + z^3\epsilon_{\alpha\beta}^{(3)}$$

$$\epsilon_{\alpha 3} = \epsilon_{\alpha 3}^{(0)} + z\epsilon_{\alpha 3}^{(1)} + z^2\epsilon_{\alpha 3}^{(3)} + z^3\epsilon_{\alpha 3}^{(3)}$$

$$\epsilon_{33} = \epsilon_{33}^{(0)} + z\epsilon_{33}^{(1)} + z^2\epsilon_{33}^{(2)}, \tag{3}$$

where

$$\epsilon_{\alpha\beta}^{(0)} = \frac{1}{2}(U_{\alpha,\beta} + U_{\beta,\alpha}) + \frac{1}{2}\frac{\partial U_3}{\partial x_\alpha}\frac{\partial U_3}{\partial x_\beta},$$

$$\epsilon_{\alpha\beta}^{(1)} = \frac{1}{2}(\phi_{\alpha,\beta} + \phi_{\beta,\alpha}),$$

$$\epsilon_{\alpha\beta}^{(2)} = \frac{1}{2}(\psi_{\alpha,\beta} + \psi_{\beta,\alpha}),$$

$$\epsilon_{\alpha\beta}^{(3)} = \frac{1}{2}(\theta_{\alpha,\beta} + \theta_{\beta,\alpha}),$$

$$\epsilon_{\alpha 3}^{(0)} = \frac{1}{2}(\phi_\alpha + U_{3,\alpha}),$$

$$\epsilon_{\alpha 3}^{(1)} = \frac{1}{2}(2\psi_\alpha + \phi_{3,\alpha}),$$

$$\epsilon_{\alpha 3}^{(2)} = \frac{1}{2}(3\theta_\alpha + \psi_{3,\alpha}),$$

$$\epsilon_{\alpha 3}^{(3)} = \theta_{3,\alpha},$$

$$\epsilon_{33}^{(0)} = \phi_3,$$

$$\epsilon_{33}^{(1)} = 2\psi_3,$$

$$\epsilon_{33}^{(2)} = 3\theta_3, \tag{4}$$

and $U_{\alpha,\beta} = \partial U_\alpha/\partial x_\beta$, $U_{3,\alpha} = \partial U_3/\partial x_\alpha$, etc. Note that the von Kármán nonlinear strains are included.

If we enforce the vanishing of shear stresses on the bounding planes of a plate, $\sigma_4(x, y \pm h/2) = 0$ and $\sigma_5(x, y \pm h/2) = 0$, we obtain

$$\phi_\alpha + U_{3,\alpha} = -\left(\frac{h}{2}\right)^2(3\theta_\alpha + \psi_{3,\alpha}),$$

$$2\psi_\alpha + \phi_{3,\alpha} = -\frac{h^2}{8}\theta_{3,\alpha},$$

or

$$\theta_\alpha = -\frac{4}{3h^2}(\phi_\alpha + U_{3,\alpha}) - \frac{1}{3}\psi_{3,\alpha},$$

$$\psi_\alpha = -\frac{h^2}{16}\theta_{3,\alpha} - \frac{1}{2}\phi_{3,\alpha}. \tag{5}$$

The displacement field in Eq. (2) becomes

$$u_\alpha = U_\alpha + z\phi_\alpha + z^2(c_1\theta_{3,\alpha} + c_2\phi_{3,\alpha}) + z^3[c_3(\phi_\alpha + U_{3,\alpha}) + c_4\psi_{3,\alpha}],$$

$$u_3 = U_3 + z\phi_3 + z^2\psi_3 + z^3\theta_3, \tag{6a}$$

where

$$c_1 = -\frac{h^2}{16}, c_2 = -\frac{1}{2}, c_3 = -\frac{4}{3h^2}, c_4 = -\frac{1}{3}. \tag{6b}$$

For the displacement field in Eq. (6a), the strains are given by Eq. (3) with the following changes:

$$\epsilon^{(2)}_{\alpha\beta} = c_1\theta_{3,\alpha\beta} + c_2\phi_{3,\alpha\beta},$$

$$\epsilon^{(3)}_{\alpha\beta} = c_3[\epsilon^{(1)}_{\alpha\beta} + U_{3,\alpha\beta}] + c_4\psi_{3,\alpha\beta},$$

$$\epsilon^{(1)}_{\alpha 3} = c_1\theta_{3,\alpha}, \epsilon^{(2)}_{\alpha 3} = 3c_3\epsilon^{(0)}_{\alpha 3}. \tag{7}$$

For a strain-consistent third-order theory of Reddy[4] we set $\theta_3 = 0$.

The principle of virtual work can be used to derive the equations of motion. The equations of motion corresponding to the displacement field (2) are:

$$N_{\alpha\beta,\beta} + f_\alpha = I_0\ddot{U}_\alpha + I_1\ddot{\phi}_\alpha + I_2\ddot{\psi}_\alpha + I_3\ddot{\theta}_\alpha,$$

$$Q_{\alpha,\alpha} + f_3 + N(U_3) = I_0\ddot{U}_3 + I_1\ddot{\phi}_3 + I_2\ddot{\psi}_3 + I_3\ddot{\theta}_3,$$

$$M_{\alpha\beta,\beta} - Q_\alpha = I_1\ddot{U}_\alpha + I_2\ddot{\phi}_\alpha + I_3\ddot{\psi}_\alpha + I_4\ddot{\theta}_\alpha,$$

$$R_{\alpha,\alpha} - P_0 = I_1\ddot{U}_3 + I_2\ddot{\phi}_3 + I_3\ddot{\psi}_3 + I_4\ddot{\theta}_3,$$

$$L_{\alpha\beta,\beta} - 2R_\alpha = I_2\ddot{U}_\alpha + I_3\ddot{\phi}_\alpha + I_4\ddot{\psi}_\alpha + I_5\ddot{\theta}_\alpha,$$

$$S_{\alpha,\alpha} - 2P_1 = I_2\ddot{U}_3 + I_3\ddot{\phi}_3 + I_4\ddot{\psi}_3 + I_5\ddot{\theta}_3,$$

$$K_{\alpha\beta,\beta} - 3S_\alpha = I_3\ddot{U}_\alpha + I_4\ddot{\phi}_\alpha + I_5\ddot{\psi}_\alpha + I_6\ddot{\theta}_\alpha,$$

$$T_{\alpha,\alpha} - 3P_2 = I_3\ddot{U}_3 + I_4\ddot{\phi}_3 + I_5\ddot{\psi}_3 + I_6\ddot{\theta}_3, \tag{8}$$

where

$$(N_{\alpha\beta}, M_{\alpha\beta}, L_{\alpha\beta}, K_{\alpha\beta}) = \int_{-h/2}^{h/2} (1, z, z^2, z^3)\sigma_{\alpha\beta}\,\mathrm{d}z, \tag{9a}$$

$$(Q_\alpha, R_\alpha, S_\alpha, T_\alpha) = \int_{-h/2}^{h/2} (1, z, z^2, z^3)\sigma_{\alpha 3}\,\mathrm{d}z, \tag{9b}$$

$$P_i = \int_{-h/2}^{h/2} (1, z, z^2)\sigma_{33}\,\mathrm{d}z$$

$$I_i = \int_{-h/2}^{h/2} \rho z^i\,dz \quad (i = 0, 1, 2, \ldots, 6) \tag{9c}$$

and ρ is the material density and

$$N(U_3) = (N_{\alpha\beta}U_{3,\beta})_{,\alpha}. \tag{10}$$

In Eqs (8) and (10), summation on repeated subscripts is assumed ($\alpha, \beta = 1, 2$). The method of moments, with weights $(1, z, z^2, z^3)$, also gives the same equation of motion.

Note that the displacement field, strains and equations of motion of the first-order shear deformation theory are obtained by setting

$$\psi_\alpha = 0, \quad \theta_\alpha = 0, \quad \phi_3 = 0, \quad \psi_3 = 0, \quad \theta_3 = 0, \tag{11}$$

in Eqs (1)–(8). The displacement field (1) of the original third-order theory of Reddy[35] is obtained by setting $\phi_3 = 0$, $\psi_3 = 0$ and $\theta_3 = 0$ in Eq. (6a).

The equations of motion associated with the displacement field (6a), according to the principal of virtual displacements, are:

$$N_{\alpha\beta,\beta} + f_\alpha = I_0\ddot{U}_\alpha + I_1\ddot{\phi}_\alpha + I_2(c_1\ddot{\sigma}_{3,\alpha} + c_2\ddot{\phi}_{3,\alpha}) + I_3[c_3(\ddot{\phi}_\alpha + \ddot{U}_{3,\alpha}) + c_4\ddot{\psi}_{3,\alpha}],$$

$$M_{\alpha\beta,\beta} + c_3K_{\alpha\beta,\beta} - (Q_\alpha + 3c_3S_\alpha) = I_1\ddot{U}_\alpha + I_2\ddot{\phi}_\alpha + I_3(c_1\ddot{\sigma}_{3,\alpha} + c_2\ddot{\phi}_{3,\alpha}) + c_3[I_3\ddot{U}_\alpha + I_5(c_1\ddot{\sigma}_{3,\alpha} + c_2\ddot{\phi}_{3,\alpha}) + I_6(c_3(\ddot{\phi}_\alpha + \ddot{U}_{3,\alpha}) + c_4\ddot{\psi}_{3,\alpha})],$$

$$-c_3K_{\alpha\beta,\alpha\beta} + Q_{\alpha,\alpha} + 3c_3S_{\alpha,\alpha} + f_3 + N(U_3) = I_0\ddot{U}_3 + I_1\ddot{\phi}_3 + I_2\ddot{\psi}_3 + I_3\ddot{\sigma}_3 - c_3[I_3\ddot{U}_{\alpha,\alpha} + I_5(c_1\ddot{\theta}_{3,\alpha\alpha} + c_2\ddot{\phi}_{3,\alpha\alpha}) + I_6(c_3(\ddot{U}_{3,\alpha\alpha} + \ddot{\phi}_{\alpha,\alpha}) + c_4\ddot{\psi}_{3,\alpha\alpha})],$$

$$-c_2L_{\alpha\beta,\alpha\beta} - P_0 = I_1\ddot{U}_3 + I_2\ddot{\phi}_3 + I_3\ddot{\psi}_3 + I_4\ddot{\theta}_3 - c_2[I_2\ddot{U}_{\alpha,\alpha} + I_3\ddot{\phi}_{\alpha,\alpha} + I_4(c_1\ddot{\theta}_{3,\alpha\alpha} + c_2\ddot{\phi}_{3,\alpha\alpha}) + I_5(c_3(\ddot{\phi}_{\alpha,\alpha} + \ddot{U}_{3,\alpha\alpha}) + c_4\ddot{\psi}_{3,\alpha\alpha})].$$

$$-c_4K_{\alpha\beta,\alpha\beta} - 2P_1 = I_2\ddot{U}_3 + I_3\ddot{\phi}_3 + I_4\ddot{\psi}_3 + I_5\ddot{\theta}_3 - c_4[I_3\ddot{U}_{\alpha,\alpha} + I_5(c_1\ddot{\theta}_{3,\alpha\alpha} + c_2\ddot{\phi}_{3,\alpha\alpha}) + c_3I_6(\ddot{\phi}_{\alpha,\alpha} + \ddot{U}_{3,\alpha\alpha}) + c_4I_6\ddot{\psi}_{3,\alpha\alpha}].$$

$$-c_1L_{\alpha\beta,\alpha\beta} + c_1R_{\alpha,\alpha} - 3P_2 = I_3\ddot{U}_3 + I_4\ddot{\phi}_3 + I_5\ddot{\psi}_3 + I_6\ddot{\theta}_3 - c_1[I_2\ddot{U}_{\alpha,\alpha} + I_4(c_1\ddot{\theta}_{3,\alpha\alpha} + c_2\ddot{\phi}_{3,\alpha\alpha}) + I_3\ddot{\phi}_{\alpha,\alpha} + I_5c_3(\ddot{\phi}_{\alpha,\alpha} + \ddot{U}_{3,\alpha\alpha}) + I_5c_4\ddot{\psi}_{3,\alpha\alpha} + I_4(c_1\ddot{\theta}_{3,\alpha\alpha} + C_2\ddot{\phi}_{3,\alpha\alpha})]. \tag{12}$$

The equations of motion of the third-order theory of Reddy[35,36] are obtained from Eqs (12) by setting $\phi_3 = 0$, $\psi_3 = 0$ and $\theta_3 = 0$.

The method of moments, with weight $(1, z, z^2, z^3)$, gives the following equations of motion:

$$
\begin{aligned}
N_{\alpha\beta,\beta} + f_\alpha &= I_0 \ddot{U}_\alpha + I_1 \ddot{\phi}_\alpha + I_2(c_1 \ddot{\theta}_{3,\alpha} + c_2 \ddot{\phi}_{3,\alpha}) \\
&\quad + I_3[c_3(\ddot{\phi}_\alpha + \ddot{U}_{3,\alpha}) + c_4 \ddot{\psi}_{3,\alpha}], \\
Q_{\alpha,\alpha} + f_3 + N(U_3) & \\
&= I_0 \ddot{U}_3 + I_1 \ddot{\phi}_3 + I_2 \ddot{\psi}_3 + I_3 \ddot{\theta}_3, \\
M_{\alpha\beta,\beta} - Q_\alpha &= I_1 \ddot{U}_\alpha + I_2 \ddot{\phi}_\alpha \\
&\quad + I_3(c_1 \ddot{\theta}_{3,\alpha} + c_2 \ddot{\phi}_{3,\alpha}) \\
&\quad + I_4[c_3(\ddot{\phi}_\alpha + \ddot{U}_{3,\alpha}) + c_4 \ddot{\psi}_{3,\alpha}], \\
R_{\alpha,\alpha} - P_0 &= I_1 \ddot{U}_3 + I_2 \ddot{\phi}_3 + I_3 \ddot{\phi}_3 + I_4 \ddot{\theta}_3, \\
S_{\alpha,\alpha} - 2P_1 &= I_2 \ddot{U}_3 + I_3 \ddot{\phi}_3 + I_4 \ddot{\psi}_3 + I_5 \ddot{\theta}_3, \\
T_{\alpha,\alpha} - 3P_2 &= I_3 \ddot{U}_3 + I_4 \ddot{\phi}_3 + I_5 \ddot{\psi}_3 + I_6 \ddot{\theta}_3, \qquad (13)
\end{aligned}
$$

which are different from Eqs (12). The equations of motion associated with the Levinson third-order theory[30] can be obtained from Eqs (13) by setting $\phi_3 = 0$, $\psi_3 = 0$ and $\theta_3 = 0$. It should be noted that Reddy's third-order theory[35] and Levinson's third-order theory[30] are different. The differences can be seen by comparing Eqs (12) with Eqs. (13).

4. COMPUTATIONAL MODELS

The displacement plate finite element models based on the first-order shear deformation theory require C^0-interpolation of all generalized displacements. The displacement-based C^0-plate elements of the first-order shear deformation plate theory are among the simplest available in the literature. Unfortunately, the accuracy of the low-order elements of this type (i.e. those with nine or fewer nodes) is less than satisfactory when span-to-thickness ratio of the elements is large. Under such circumstances, the shearing strains are required to vanish, and the plate elements based on the first-order theory become excessively stiff, yielding displacements that are too small compared to the true solution. This type of behavior, known as *shear locking*, has plagued shear deformable elements since their inception (see Refs 71, 72).

Shear locking is due to the inability of shear deformable elements to accurately model the curvatures within an element under a state of zero transverse shearing strain. This argument may be modified and extended to account for membrane locking in curved elements, as well as the poor behavior of all elements which contain multi-strain fields (e.g. plane stress and plane strain elements). The various means employed to alleviate shear locking in plate elements include reduced integration,[71–73] mixed formulations,[74,75] hybrid formulations,[76] assumed strain techniques,[77] and discrete Kirchhoff methods,[78] to name only a few. Of the large number of new displacement-based elements in the literature, only a few have been reasonably successful,[73–75] and there is still much room for improvement in terms of accuracy, ease of implementation, and computational efficiency.

After many unsuccesful attempts to develop a general plate element, it became clear to many researchers that a better understanding of locking phenomena and the effects of reduced integration was necessary in order to give guidelines for the development of new elements and to allow a more complete anlaysis of existing elements. As the span-to-thickness ratio of a plate tends towards a large number, a constraint condition is imposed which requires the product of the shear stiffness matrix and the displacement vector to be zero. Therefore, in order to obtain a non-trivial solution, it was concluded that the shear stiffness matrix must be singular. These observations led to explanations of locking behavior based upon measures of singularity of the shear stiffness matrix,[79,80] the number of independent shear constraints imposed on an element in the thin plate limit, and other criteria. Prathap and Bhashyam[81] demonstrated that locking is a function of the type of constraints that arise when an element is very thin. These investigators developed a method of identifying the actual constraints that arise under full or reduced integration, and, by deriving the constraints in terms of the nodal degrees of freedom, were able to classify them as being either proper Kirchhoff constraints that enforce a condition of zero transverse shearing strain or spurious constraints that cause locking. Prathap and his coworkers have also contributed significantly to the understanding of locking, field-consistency, and stress oscillations in finite element models of beams, plates, and shells.

Recently, Averill and Reddy[4,5] presented a new analytical technique for identifying the exact form of the shear constraints that are imposed on an element when its side-to-thickness ratio is very large. The technique yields results that are equivalent to those obtained by Prathap and Bhashyam[81] for Timoshenko beam elements, but the method of Averill and Reddy[4] is much simpler both in concept and in application to two-dimensional elements, especially when high orders of interpolation and/or Gaussian quadrature are employed. By applying the technique to several popular plate elements based on the first-order theory, it was shown by Prathap and Bhashyan[81] that, if the form of the shear constraints in an element are known, the performance of that element when used to model thin structures can be determined *a priori*. Furthermore, by studying the form of the constraints, a more complete understanding of the locking behavior of plate elements was gained, resulting in new insights and definitive conclusions regarding the origin of locking phenomena and the effects of reduced integration.

The displacement finite element models of higher-order theories can be C^0 type if the displacement expansions do not contain the derivatives of the transverse displacement. For example, displacement expansions of the type in Eq. (2) require C^0-interpolation of the variables U_α, U_3, ϕ_α, ψ_α, θ_α, ϕ_3, ψ_3 and θ_3. Such models were developed by Kant and his colleagues.[59-61] If vanishing of transverse shearing strains on plate surfaces is the displacement field is written in terms of the derivatives of the transverse displacement ($u_{3,\alpha}$), as shown in Eq. (6a). The displacement finite models of the theories based on the displacement field (6a) or its equivalent, require C^1-interpolation of the variables U_3, ϕ_3, ψ_3, and θ_3, and C^0-interpolation of the other variables. Such models have been developed in Refs 5, 63–65. A mixed formulation of these theories require C^0-interpolation of all generalized displacements and stress resultants (see Refs 66–68).

The application of the technique of Averill and Reddy[4] for identifying shear constraints has been applied in Ref. 5 to plate elements based on a generalized form of the third-order theory of plate bending presented by Reddy.[35,36] Third-order shear deformation plate theories and their associated plate finite elements have been much maligned in the past due to the misconception that their formulation and implementation are overly complicated and that their use is unjustifiably expensive. In order to clear up this misconception, Averill and Reddy[5] demonstrated through numerous numerical examples that selected elements based upon third-order plate theories not only are comparable, and in some cases superior, to the best Mindlin-type elements in terms of accuracy, but also they are extremely efficient in terms of computational cost. A summary of this development is presented here.

Consider the displacement field for the third-order theory of Reddy,[35,36] which is obtained from Eq. (2) by setting $\phi_\alpha = \hat{\phi}_\alpha - U_{3,\alpha}$, $\phi_3 = 0$, $\psi_3 = 0$, and $\theta_3 = 0$:

$$u_\alpha = U_\alpha - zU_{3,\alpha} + z\left[1 - \frac{4}{3}\left[\frac{z}{h}\right]^2\right]\hat{\phi}_\alpha, \quad u_3 = U_3 \tag{14}$$

where (U_α, U_3) are displacements of the mid-surface of the plate in the x_α and z directions, respectively. The different forms of the displacement field are obtained by making the appropriate change of variables for the generalized rotations $\hat{\phi}_\alpha$ (see Reddy[3]).

The equilbrium equations of the linear theory associated with the displacement field (14) are:

$$N_{\alpha\beta,\beta} f_\alpha = 0, \quad -M_{\alpha\beta,\alpha\beta} + N(U_3) + f_3 = 0,$$

$$M_{\alpha\beta,\beta} + c_3 K_{\alpha\beta,\beta} - (Q_\alpha + 3c_3 S_\alpha) = 0, \tag{15}$$

where $N_{\alpha\beta}$, $M_{\alpha\beta}$, $K_{\alpha\beta}$, Q_α and S_α are the resultants defined in Eq. (9).

As discussed in Refs 4 and 80, it is illuminating to rewrite the potential energy for the special case of uniform, isotropic plates in terms of new, nondimensional variables. The nondimensionalized potential energy takes the form:

$$\Pi = Eh^3\{\bar{U}_b + \lambda \bar{U}_s\} \tag{16a}$$

$$\lambda = \frac{G}{E}\left(\frac{a}{h}\right)^2 \tag{16b}$$

where E is Young's modulus, G is the shearing modulus, a is the length along a side of the plate, and h is the thickness of the plate. The energy related to transverse shear is given by

$$\bar{U}_s = \frac{1}{2}\int_\Omega \frac{8}{15}\hat{\phi}_\alpha \hat{\phi}_\alpha \, d\bar{x}\, d\bar{y} \tag{17}$$

where $\bar{x}$ and $\bar{y}$ are the nondimensional mid-plane coordinates. As can be seen in Eq. (16), the shearing energy is prefixed by a term, λ, which behaves as a penalty parameter.[51,52] This term tends towards infinity as the plate thickness is decreased, and, in the thin plate limit (i.e. as $a/h \to \infty$), the penalty parameter enforces the Kirchhoff constraints:

$$\hat{\phi}_\alpha = 0 \quad (\alpha = 1, 2). \tag{18}$$

The finite element model obtained by minimizing the potential energy in Eq. (16) can be written as:

$$([\bar{\mathbf{K}}_b] + \lambda[\bar{\mathbf{K}}_s])\{\bar{\mathbf{u}}\} = \{\bar{\mathbf{F}}\}, \tag{19}$$

where $[\bar{\mathbf{K}}_b]$ is the bending stiffness matrix, $[\bar{\mathbf{K}}_s]$ is the shearing stiffness matrix, $\{\bar{\mathbf{u}}\}$ is the displacement vector, and $\{\bar{\mathbf{F}}\}$ is the load vector. In the thin plate limit (i.e. when λ tends towards infinity), $[\bar{\mathbf{K}}_s]\ \{\bar{\mathbf{u}}\}$ must vanish identically in order for the potential energy to remain bounded. This is equivalent to satisfying the Kirchhoff constraints in Eq. (18), which implies that the shearing strain in each element should vanish as its thickness is decreased. Furthermore, each element must be able to model a state of zero transverse shearing strain without adversely modifying the form of the bending energy. The inability of an element to fulfill this requirement leads to the behavior known as locking. Fortunately, it is now possible to predict *a priori* whether or not an element will lock in thin plate applications, so that reliable elements may be identified.

The technique presented by Averill and Reddy[4] for determining the exact form of the shearing constraints in thin shear deformable elements can be employed to predict the behavior of elements based upon the generalized form of Reddy's third-order plate theory. In the finite element model, the Kirchhoff constraints in Eq. (18) are approximated within each element according to the assumed form of the displacement field and the interpolation functions used to approximate each variable. For example, the constraints imposed on a thin element which utilizes the same displacement field as Reddy[35] [see Eq. (2)] are:

$$\sum_{i=1}^{m} \phi_\alpha^i M_i + \sum_{i=1}^{n} U_3^i \frac{\partial N_i}{\partial x_\alpha} = 0 \quad (\alpha = 1, 2), \tag{20}$$

where ϕ_α^i and U_3^i are the rotations and the transverse deflection at the ith nodal point, and M_i and N_i are the interpolation functions for the rotations and transverse deflection, respectively. The conditions in Eq. (20) must be satisfied exactly at the Gaussian integration points that are used to integrate the shearing stiffness matrix. Thus, we have:

$$\sum_{i=1}^{m} \phi_\alpha^i M_i(x_\alpha^k) + \sum_{i=1}^{n} U_\alpha^i \frac{\partial N_i(x_\alpha^k)}{\partial x_\alpha} = 0 \quad (\alpha = 1, 2), \tag{21}$$

for $k = 1, 2, \ldots, NGP$, where NGP is the number of Gauss points and x_α^k are the coordinates of the kth Gauss point. By expanding Eq. (21) and performing the necessary algebraic simplifications, the shearing constraints can be interpreted as discretized equivalents of either the true Kirchhoff constraints or some other condition that will cause locking (see Ref. 5).

As an example we consider the element described above based on the displacement field used by Phan and Reddy[63] and in which U_3 is approximated by the nonconforming cubic interpolation functions of Melosh[82], while the variation of ϕ_α is governed by the Lagrangian bilinear interpolation functions. When the stiffness coefficients are integrated exactly (i.e. using a 4×4 mesh of integration points), the following shear constraints arise:

$$\phi_\alpha^i + \theta_\alpha^i = 0 \quad (i = 1, 2, 3, 4), \tag{22}$$

$$\frac{U_3^{i+1} - U_3^i}{a} = \frac{\theta_\alpha^{i+1} + \theta_\alpha^i}{2} \quad (\alpha = 1; i = 1, 3), \tag{23}$$

$$\frac{U_3^{i+2} - U_3^i}{b} = \frac{\theta_\alpha^{i+2} + \theta_\alpha^i}{2} \quad (\alpha = 2; i = 1, 2), \tag{24}$$

$$\theta_\alpha^{i+2} - \theta_\alpha^i = \theta_\alpha^{i+3} - \theta_\alpha^{i+1} \quad (\alpha = 1, 2), \tag{25}$$

where

$$\theta_{\alpha i} = U_{3,\alpha}|_{x_\alpha^i}, \tag{26}$$

and x_α^i are the coordinates of the ith node. The four sets of expressions (22) are true Kirchhoff constraints which relate the rotations ϕ_α to the slopes $U_{3,\alpha}$. However, the remaining constraints Eqs (23–25) contain only terms which appear in the approximation of U_3. The effect of these constraints is to restrict the originally cubic variation of the transverse deflection to a quadratic one. At the element level, this implies that the curvature strains are constant, as is the case for four noded Mindlin-type elements. At the global level, however, the slopes are required to be continuous at the nodes and tangential to (but not normal to) the inter-element boundaries, which imposes additional constraints on the approximation of the deflection. While it is possible for the slopes to be continuous when the deflection varies quadratically, the resulting solution will not likely resemble the true solution, so that the results obtained in practice will always be too stiff. It should be noted, however, that the locking constraints, Eq. (25), and two of the four constraints, Eq. (23), are satisfied exactly for the case of cylindrical bending, so that the element may be expected to give better results for this type of deformation than for deformations which involve curvature about two axes.

The use of a 2×2 integration rule to evaluate the stiffness coefficients yields only limited improvement in the thin plate modeling capabilities and a 3×3 rule gives no improvement at all. The shear constraints that are present in this case are given in Ref. 83, where it is shown that the locking constraints are less severe than in the exactly integrated element, but still cause the element to be too stiff when used to model thin structures. The shear constraints for a conforming element are also given in Ref. 83. These constraints, while slightly different in form, lead to the same conclusions regarding locking behavior in thin plate applications. Numerical examples will be presented in the next section to verify these predictions of element behavior based on the form of the shear constraints.

It has been shown by many researchers that the shearing strains must be interpolated consistently in order to eliminate all spurious stiffness effects (see Refs 81, 83). For the element just discussed, a consistent interpolation scheme would be one in which the rotations ϕ_α vary according to the derivatives of the deflection field $U_{3,\alpha}$ ($\alpha = 1, 2$). While such an interpolation scheme is possible, it would be inconvenient to implement and would lead to a computationally inefficient element. Therefore, a new approach should be sought.

A more desirable consistent finite element approximation of the shearing strains is easily identified by examining the generalized form of the shearing strains in (3). The consistency criteria may be satisfied identically by using the generalized rotations $\hat{\phi}_\alpha$. If these rotational degrees of freedom are then approximated by the bilinear Lagrangian interpolation functions, the shear constraints which arise in thin elements are:

$$\hat{\phi}_\alpha^i = 0 \quad \text{for } i = 1, 2, 3, 4. \tag{27}$$

When these constraints are enforced, the shearing energy will vanish, and the bending energy will reduce precisely to that of the classical plate theory. This form of the third-order theory was first used by

Bhimaraddi and Stevens,[37] and a finite element based upon this form was developed by Ren and Hinton.[64] The latter investigators demonstrated that their plate element does not lock at all in thin plate applications, and yields accurate results for both thick and thin rectangular plate structures. This element employs the non-conforming cubic interpolation functions of Melosh[82] for approximating the transverse deflection and the bilinear Lagrange interpolation functions for the rotational degrees of freedom. A 4×4 Gaussian integration rule is required to integrate the stiffness coefficients exactly. While the element has been shown to behave well in thick and thin geometries, its sensitivity to distortion and its computational efficiency have yet to be investigated. Perhaps this is why the element has not yet received widespread acclaim.

5. NUMERICAL EVALUATION OF THE ELEMENTS

In this section, the overall behavior of several shear deformable plate elements is discussed in light of the results of the paper.[5] The criteria to be tested are: accuracy, distortion sensitivity, efficiency, and rank sufficiency. Each of the elements to be tested allows for a linear distribution of the strain components within the element.

Of the Reddy-type elements that are evaluated, four are based on the original theory of Reddy,[35] and four are based on the theory in Ref. 3 [see Eq. (14)] in which $\hat{\phi}_\alpha$ are used in place of ϕ_α. The notation used to designate these elements is as follows. The number preceding the name specifies the number of nodes in the element (always four in this study). The following three or four letters describe the theory upon which the element is based (RED for Reddy's theory and MRED for the modified form of the theory in which $\hat{\phi}_\alpha = \phi_\alpha$). The final one or two letters before the hyphen denote whether the element is conforming (C) or nonconforming (NC). Lastly, the letter after the hyphen describes the type of integration used to evaluate the stiffness coefficients (F for a uniform 4×4 mesh of full integration points and R for a uniformly reduced 2×2 mesh). For example, 4MREDC-F and 4MREDNC-R are the conforming and nonconforming elements based on the modified form of Reddy's theory which employ uniform full (4×4) and reduced (2×2) integrations, respectively.

Many elements based on the first-order plate theory have been developed and tested, but none surpass the overall accuracy and economy of the Lagrangian nine-noded element with selectively-reduced integration[80] (hereafter called the 9MIN-S element). This element contains one zero energy mode, which precludes its use in general purpose finite element codes, but it is well suited for benchmark testing. For this reason, the 9MIN-S element has been chosen by the authors as the standard element against which the merits (i.e. accuracy and efficiency) of other elements should be measured. The other Mindlin-type element to be tested is the heterosis element with selectively-reduced integration,[84] and denoted by 9HET-S. The reasons for the excellent behavior of these two elements has been explained in detail[4] based upon the form of the shear constraints that arise in thin element situations.

A numerical procedure that can be used to immediately screen out many elements (and to discover new ones, as will be seen) is the elemental stiffness rank test. An eigenvalue analysis of the stiffness matrix of the element is performed in order to determine the number of zero energy modes which are present under various numerical integration rules. The results are presented in Table 1. The elemental stiffness matrix $[\mathbf{K}] = [\mathbf{K}_b] + [\mathbf{K}_s]$ should contain three zero eigenvalues, which correspond to the rigid body modes. Any additional zero eigenvalues are due to zero energy nodes or mechanisms. It is often stated that certain zero energy modes are eliminated in the assembled stiffness matrix by the application of appropriate boundary conditions. However, experience has shown that, in plates with constrained interior boundaries such as holes and in many linear buckling problems (see the section on buckling analysis), zero energy modes may contaminate the solution despite sufficiently constrained exterior boundaries. Thus, elements which possess a rank deficient stiffness matrix should be avoided altogether in general purpose finite element program unless care has been

Table 1. Eigenvalue analysis of the Reddy-type elements[5]

Element D.O.F. per node	Numerical integration grid: Name of integration rule	Bending terms	Transverse shearing terms	Number of zero eigenvalues: K_s	$K_b + K_s$
4REDC	Full	4×4	4×4	6	3
$w\ w_{,x}\ w_{,y}\ w_{,xy}$	Selective	4×4	2×2	16	3
$\psi_x\ \psi_y$	Reduced	2×2	2×2	16	3
4REDNC	Full	4×4	4×4	6	3
$w\ w_{,x}\ w_{,y}$	Selective	4×4	2×2	12	3
$\psi_x\ \psi_y$	Reduced	2×2	2×2	12	3
4MREDC	Full	4×4	4×4	16	3
$w\ w_{,x}\ w_{,y}\ w_{,xy}$	Selective	4×4	2×2	16	3
$\varphi_x \varphi_y$	Reduced	2×2	2×2	16	4
4MREDNC	Full	4×4	4×4	12	3
$w\ w_{,x}\ w_{,y}$	Selective	4×4	2×2	12	3
$\varphi_x\ \varphi_y$	Reduced	2×2	2×2	12	3

taken to suppress all possible mechanisms. As seen in Table 1, a fortuitous property exists in all but one of the Reddy-type elements. That is, the entire stiffness matrix may be integrated by a uniform 2×2 integration rule without the introduction of zero energy modes. This property is easily explained by noting that nearly all of the terms in the stiffness matrix are integrated exactly by the 2×2 rule. Only a few of the terms in the bending stiffness matrix and in the mass and stability matrices will be approximated by performing the integrations in this way. Furthermore, the 2×2 integration points correspond to the optimum strain sampling points for the C^1-cubic interpolation functions.[82] It will be demonstrated below that the elements which utilize 4×4 and 2×2 integration rules yield nearly identical results. Thus, the application of reduced integration to these elements should not be looked upon as a trick, but simply as a mild approximation which reduces the stiffness computation time by as much as 75 per cent. These elements will be evaluated and discussed further in the sequel.

To assess the behavior of the elements in a variety of applications, problems of plate bending are analyzed for assorted boundary conditions and material properties. The two types of materials used are:

$$\text{material 1:} \quad E = 10.0 \times 10^6, \quad \nu = 0.3, \quad \rho = 1;$$

$$\text{material 2:} \quad E_1 = 25.0 \times 10^6, \quad E_2 = 1.0 \times 10^6,$$

$$G_{12} = G_{13} = 0.5 \times 10^6, \quad G_{23} = 0.2 \times 10^6,$$

$$\nu_{12} = \nu_{13} = 0.25, \quad \rho = 1.$$

Computations were carried out in double precision on an IBM 3090 computer. All results are normalized by the exact solution of the problem discussed.

The first two numerical examples are designed to assess the ability of the elements to model thin plate structures and thus to verify the role that shear constraints play in determining the behavior of thin shear deformable elements. The deflections of a cantilever isotropic beam under a tip load and a clamped isotropic plate under a uniform load are investigated for a wide range of plate span-to-thickness ratios. For the cantilever beam, a 5×1 mesh of elements is used, and a 4×4 mesh is employed for a quarter model of the clamped plate. All results are normalized by the exact solutions for thin plates.[14] These standard test cases demonstrate the behavior of thin plate elements in deformations with single and double curvature, respectively. It can be seen in Tables 2 and 3 that all of the elements considered yield excellent results except for those based on the original form of Reddy's theory, which does not employ consistent interpolation of the shearing strains. When used to model the cantilever beam, these elements exhibit a small amount of excess stiffness due to the spurious constraints. However,

Table 2. Normalized tip deflection of an isotropic, cantilever beam with an end load[5]

a/h	9MIN-S	9HET-S	4REDC-F	4REDC-R	4REDNC-F	4REDNC-R	4MREDC-F	4MREDNC-F	4MREDNC-R
5	1.024	1.023	1.010	1.014	1.009	1.013	1.012	1.012	1.012
10	1.000	0.999	0.984	0.990	0.984	0.989	0.989	0.990	0.990
50	0.993	0.986	0.971	0.975	0.972	0.976	0.981	0.982	0.982
100	0.993	0.985	0.965	0.969	0.966	0.975	0.981	0.982	0.982
500	0.993	0.984	0.929	0.941	0.932	0.974	0.981	0.982	0.982
1000	0.993	0.984	0.915	0.936	0.917	0.974	0.981	0.982	0.982

Table 3. Normalized center deflection of an isotropic, clamped plate subjected to a uniform load[5]

a/h	9MIN-S	9HET-S	4REDC-F	4REDC-R	4REDNC-F	4REDNC-R	4MREDC-F	4MREDNC-F	4MREDNC-R
5	1.725	1.724	1.662	1.682	1.666	1.686	1.600	1.635	1.635
10	1.195	1.194	1.159	1.186	1.163	1.190	1.167	1.191	1.191
50	1.013	1.011	0.922	0.946	0.926	0.946	1.022	1.041	1.041
100	1.007	1.003	0.818	0.879	0.818	0.872	1.017	1.036	1.036
500	1.005	0.998	0.199	0.373	0.190	0.318	1.016	1.035	1.035
1000	1.005	0.998	0.060	0.140	0.056	0.110	1.015	1.035	1.035

the elements lock completely when modeling the clamped plate. These results are in complete agreement with the predictions made in the previous section based on the form of the shearing constraints. Because the elements based on the original form of the theory behave poorly when applied to thin structures, they will not be considered further.

Next, the accuracy of the remaining elements in modeling the bending of simply-supported laminated plates will be investigated. Table 4 shows the results of a square (0/90/90/0) laminate subjected to a sinusoidal load for two values of the plate span-to-thickness ratio. For a coordinate system with its origin at a corner of the plate, the following normalized deflection and stresses are given:

$$\bar{w}\left(\frac{a}{2},\frac{a}{2},0\right),\quad \bar{\sigma}_x\left(\frac{a}{2},\frac{a}{2},\frac{h}{2}\right),\quad \bar{\sigma}_y\left(\frac{a}{2},\frac{a}{2},\frac{h}{4}\right),$$

$$\bar{\sigma}_{xy}\left(0,0,\frac{h}{2}\right),\quad \bar{\sigma}_{yz}\left(\frac{a}{2},0,0\right),\quad \bar{\sigma}_{xz}\left(0,\frac{a}{2},0\right),$$

where the results are normalized by the exact solution of Phan and Reddy.[61] The stresses are computed in each element at the reduced integration point nearest the desired location in the plate. For $a/h = 100$, the Mindlin-type elements yield the most accurate deflections, while the most accurate in-plane stresses are given by the Reddy-type elements, especially 4MREDNC-F and 4MREDNC-R, which give nearly identical results. For the thicker plate, $a/h = 10$, the solution given by the Mindlin-type elements seems to converge to about 7–10 per cent below the closed form solution. The Reddy-type elements, on the other hand, yield excellent results for nearly all stresses and displacements, converging rapidly from above in each case. The prediction of $\bar{\sigma}_{xy}$ given by MREDC-F is less than satisfactory, but no explanation for this single anomolous result can be provided. Because the Mindlin theory accounts for only a constant value of transverse shearing strain through the thickness of the plate, it is not capable of predicting accurate values of the transverse shearing stresses via the constitutive equations. However, Reddy's theory, and the associated finite elements, predict very accurately the transverse shearing stresses due to the parabolic variation of transverse shearing strains through the thickness. The 4MREDNC-F and 4MREDNC-R elements give extremely accurate results for all of the stress values, even for a course 2×2 mesh. It should be emphasized that for a value of span-to-thickness ratio that is usually associated with thin plate behavior, $a/h = 10$, the Mindlin-type elements are still not capable of capturing the appropriate in-plane deformations (and hence stresses) for this laminate.

Next, we will turn our attention to two element properties—distortion sensitivity and computational efficiency. A subparametric formulation is employed, where the bilinear interpolation functions are used

Table 4. Maximum deflection and stresses in a simply-supported (0/90/90/0) laminate subjected to a sinusoidal load (material 2)[5]

a/h	Element	Mesh	$\bar{W}$	$\bar{\sigma}_x$	$\bar{\sigma}_y$	$\bar{\sigma}_{xy}$	$\bar{\sigma}_{yz}$	$\bar{\sigma}_{xz}$
	9MIN-S	2×2	0.928	0.888	0.903	0.869	0.878	0.613
		4×4	0.927	0.908	0.923	0.894	0.897	0.627
	9HET-S	2×2	0.926	0.888	0.903	0.869	0.878	0.613
		4×4	0.927	0.908	0.923	0.894	0.897	0.627
10	4MREDC-F	2×2	1.033	1.046	1.001	0.817	1.049	0.926
		4×4	1.004	1.019	1.001	0.768	1.082	0.989
	4MREDNC-F	2×2	1.094	1.007	1.005	1.080	1.099	1.016
		4×4	1.024	1.002	1.003	1.021	1.076	1.004
	4MREDNC-R	2×2	1.094	1.008	1.007	1.080	1.098	1.016
		4×4	1.024	1.002	1.003	1.021	1.076	1.004
	9MIN-S	2×2	0.999	0.970	0.969	0.971	0.873	0.593
		4×4	0.999	0.992	0.992	0.993	0.896	0.609
	9HET-S	2×2	0.995	0.968	0.968	0.969	0.898	0.598
		4×4	0.998	0.992	0.992	0.993	0.896	0.610
100	4MREDC-F	2×2	1.089	1.055	1.056	0.912	1.096	0.953
		4×4	1.013	1.023	1.010	0.895	1.021	0.990
	4MREDNC-F	2×2	1.097	1.014	1.006	1.060	1.034	1.018
		4×4	1.024	1.004	1.004	1.018	1.007	1.005
	4MREDNC-R	2×2	1.097	1.014	1.008	1.060	1.032	1.018
		4×4	1.024	1.004	1.004	1.018	1.006	1.005

for the coordinate transformation and for the approximation of the generalized rotations $\hat{\phi}_\alpha$. The transverse deflection is approximated by either bicubic conforming or cubic nonconforming functions. In all cases, the interpolation functions are given in the local (or natural) coordinates.

In order to determine how accurate the elements are in nonrectangular configurations, the distorted meshes in Fig. 1 are to be used to analyze a clamped, isotropic plate with a concentrated load at the center of the plate. Again, results are normalized by the exact solution for thin plates.[14] Figure 2 shows that the 9MIN-S element is virtually oblivious to the mesh distortions. The excellent results for this isoparametric element casts doubts on the true effect of the assumed natural coordinate strain formulations,[77] which claim to yield superior results for distorted meshes. The behavior of 9HET-S is more than satisfactory, but not as good as 9MIN-S. The 4MREDNC-R element yields very good results for an angle of distortion up to 30°, with the other Reddy-type elements giving slightly inferior results. The behavior of these elements when the angle $\theta = 40°$ is a little less than satisfactory, but this is indeed an extreme case which would not (or should not) be encountered in most analyses. The superior behavior of the Mindlin-type elements over the Reddy-type elements in this example may be at-

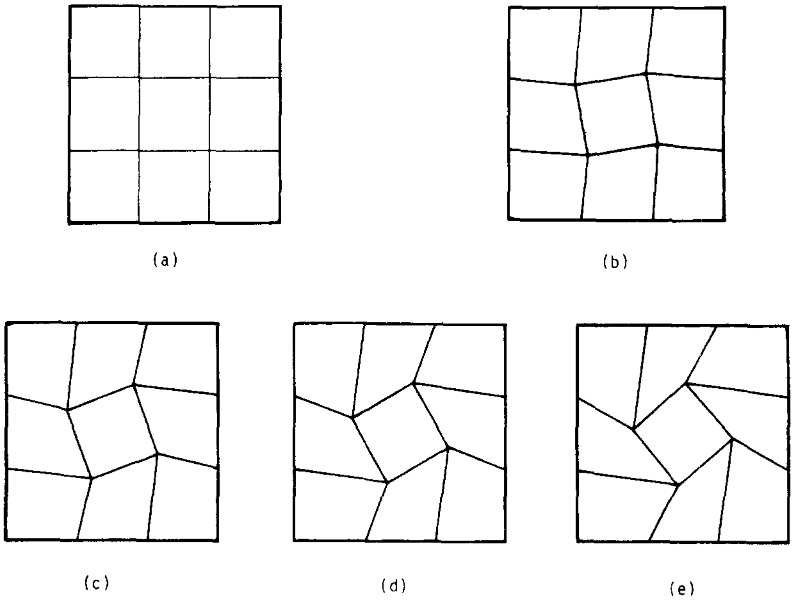

Fig. 1. The 3×3 meshes used to investigate the distortion sensitivity. (a) Undistorted, (b) $\theta = 10$, (c) $\theta = 20$, (d) $\theta = 30$, and (e) $\theta = 40$.

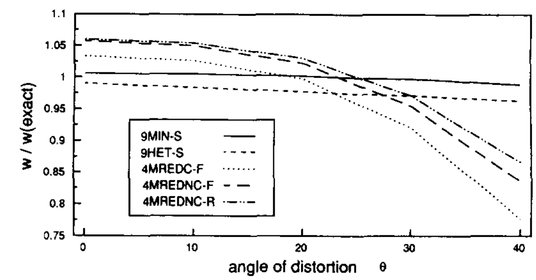

Fig. 2. Effect of mesh distortion on the modeling of a clamped isotropic plate with concentrated load at the centre.

tributed to the higher order of geometric modeling in the nine-noded Mindlin-type elements compared to the four-noded Reddy-type elements.

In order to assess the efficiency of each element, the problem of the simply-supported (0/90/90/0) laminate under a sinusoidal load is revisited, with the VS FORTRAN Version II Interactive Debugger (IAD)[85] being employed to determine the execution time for each subroutine in the finite element programs. IAD samples the program every 10 ms during execution to record the statement being executed. Because a sample interval of 10 ms is not small enough to measure precise execution times, the results of this test should not be interpreted as being exact. However, the amount of error is not enough to skew the outcome even slightly, making this test a good measure of the relative efficiency of the elements. The two programs written for the Mindlin and Reddy-type finite element models are essentially identical, except for the computation of the stiffness matrices and some parts of the pre- and post-processing. The solution is obtained using a banded equation solving routine. Results are presented in Table 5 for two sizes of the mesh. Because the Reddy-type elements all have only four nodes, the bandwidth and the total number of equations is less in these elements than in the nine-noded Mindlin-type elements. Thus, the CPU time required to solve the assembled set of equations is approximately four to eight times less for the same size meshes of elements based on the third-order theory than the meshes of the Mindlin-type elements. As far as computation of the elemental stiffness matrices and assembly of the global system of equations is concerned, the Mindlin-type elements are substantially more efficient than the exactly integrated Reddy-type elements. However, it is seen that a nearly 75 per cent savings in assembly time can be obtained by using reduced integration to evaluate the elemental stiffness coefficients instead of an exact integration rule, making assembly of the 4MREDNC-R element much less than that of either 9MIN-S or 9HET-S. Thus, for the 4×4 mesh, the 4MREDNC-R element requires less than half the total CPU time of its nearest competitor, 9HET-S, and this ratio decreases to just above one-quarter for the 6×6 mesh. For the larger mesh, the 4MREDNC-F element is also cheaper than either of the Mindlin-type elements, but still 2.5 times more expensive than its reduced-integrated counterpart. It is interesting to note that the 4×4 mesh of 9MIN-S elements and the 6×6 mesh of 4MREDNC-R elements have approximately the same number of total equations, and the model with 4MREDNC-R elements is still the least expensive of the two. Therefore, the prevailing conclusion that elements based on the third-order theory (and requiring C^1 continuity) are unduly expensive is proven to be incorrect.

6. IMPLEMENTATION AND USE OF REFINED PLATE ELEMENTS

The overall accuracy and efficiency of the 4MREDNC-F and 4MREDNC-R plate elements have been firmly established, but questions remain about the convenience of using these elements in general purpose programs. One of the main obstacles is the fact that these elements have five bending degrees of freedom per node, instead of the usual three engineering degrees freedom—one deflection and two rotations. Because the refined elements require C^1-continuity of the transverse deflection, there are two additional rotational degrees of freedom corresponding to the derivatives of the deflec-

Table 5. CPU time (seconds) required to evaluate the structure in Table 3[5]

Mesh		9MIN-S	9HET-S	4MREDC-F	4MREDNC-F	4MREDNC-R
	Total nodes	81	81	25	25	25
	Total equations	243	227	150	125	125
	Half bandwidth	63	59	42	35	35
4×4	$\bar{w}$	0.999	0.998	1.013	1.024	1.024
	Time to assemble (s)	0.54	0.46	1.50	1.07	0.29
	Time to solve (s)	0.76	0.62	0.27	0.16	0.16
	Total CPU time (s)	1.36	1.15	1.79	1.26	0.47
	Total nodes	169	169	49	49	49
	Total equations	507	471	294	245	245
	Half bandwidth	87	81	54	45	45
6×6	$\bar{w}$	0.999	0.999	1.003	1.001	1.011
	Time to assemble (s)	1.24	1.20	3.36	2.41	0.64
	Time to solve (s)	3.26	2.60	0.74	0.42	0.42
	Total CPU time (s)	4.61	3.93	4.16	2.87	1.11

tion. In this section, it will be shown how this problem can be overcome and be viewed as an advantage instead of a hindrance.

It is common for the user of a commercial finite element code to be unaware of all the details involved in the computation and assembly of a finite element stiffness matrix. Likewise, the user need not worry about every step taken during the preprocessing portion of a program. Therefore, it is proposed that two of the four rotational degrees of freedom may be "invisible" to the user. This causes no problem with the application of boundary conditions, because there are no conceivable cases where one member of the two sets of rotations ($U_{3,\alpha}$, $\hat{\phi}_\alpha$) will be constrained without the status of the other also being implied. This is clear from the form of the boundary conditions given in Eq. (7), where it is seen that if M_{11} is unknown, both $\hat{\phi}_1$ and $U_{3,1}$ must be specified, and likewise for the respective x_2-components. Therefore, either both members of a set of rotations must be specified as boundary conditions, or neither member can be specified (when the applied moment is known). In most problems, both members of a set of rotations will be constrained to zero due to conditions at the boundary of a structure. In this case, when the one "visible" member of the set of rotations is constrained to zero, a simple preprocessing step can add this boundary condition to the other member. In the case where the slope, $\partial U_3/\partial n$, of a boundary must be specified as some nonzero quantity, the additional rotation, $\hat{\phi}_n$, must be specified as zero at that point. Therefore, it is suggested that the "visible" rotations be the familiar slopes of the deflection, and the "invisible" rotations, which can be specified during preprocessing based on the other boundary conditions, be the $\hat{\phi}_\alpha$ degrees of freedom. The same technique can be employed when a force boundary condition, a moment in this case, is applied. According to the variationally consistent form of the boundary conditions the value of the moment should be added to the force vector in the equations corresponding to both members of the set of rotations that are in the same direction as the moment. Again, this modification can be made to the boundary condition data during preprocessing.

It should be noted that $\hat{\phi}_\alpha$ are not true rotations, but are actually measures of the transverse shearing strain. Therefore, when $\hat{\phi}_\alpha$ are specified to be zero, as at clamped boundaries, the shearing strain is automatically zero at these points. This is an unfortunate property of the plate theory, but it clearly has no deleterious effects on the numerical results, as seen herein.

When using refined plate theories or their associated finite element models, questions often emerge about the meaning of the higher-order stress resultants such as $K_{\alpha\beta}$, and R_α, in Eq. (9). These terms arise naturally in the variational formulation of the theory and must be included, but their physical meaning and significance are difficult to interpret. The one thing that is understood is that these types of loads are not applied externally to engineering structures. Therefore, it is customary to simply assume that they are either zero or unknown (when the corresponding displacement is specified). In this way, the question of their physical meaning need not be addressed directly, with the understanding that they are a necessary component of the mathematical formulation of the problem.

As a final note, the 4MREDNC-R element appears to be ideally suited to be used as a flat, four-noded shell element for applications in which the membrane and bending coupling are not significant. The entire elemental stiffness matrix (membrane, bending, and shearing portions) may be integrated using a uniform 2×2 rule, yielding a very efficient and accurate element.

Acknowledgement—The support of this research by NASA through Grants NGT-50404 and NAG-1-1030 is gratefully acknowledged.

REFERENCES

1. J. N. Reddy, "On refined computational models of composite laminates," *International Journal of Numerical Methods in Engineering* **27**, 361–382 (1989).
2. J. N. Reddy, "A review of refined theories of laminated plates," *The Shock and Vibration Digest* **22**(7), 3–17 (1990).
3. J. N. Reddy, "A general non-linear third-order theory of plates with transverse shear deformation," *Journal of Non-Linear Mechanics* **25**(6), 677–686 (1990).
4. R. C. Averill and J. N. Reddy, "On the behavior of plate elements based on the first-order shear deformation theory," *Engineering Computing* **7**(1), 57–74 (1990).
5. R. C. Averill and J. N. Reddy, "An assessment of shear deformable plate finite elements," *International Journal of Numerical Methods in Engineering*, in press.
6. A. V. Krishna Murty, "Theoretical modelling of laminated composites plates," in *Composite Materials and Structures* (edited by K. A. V. Pandalai), pp. 85–93, Tata McGraw-Hill, New Delhi, India, 1988.
7. M. Sathyamoorthy, "Effects of transverse shear and rotatory inertia on large amplitude vibration composite plates and shells," *Composite Materials and Structures* (edited by K. A. V. Pandali), pp. 95–105, Tata McGraw-Hill, New Delhi, India, 1988.
8. R. K. Kapania and S. Raciti, "Recent advances in analysis of laminated beams and plates, part I: shear effects and buckling," *AIAA Journal* **27**(7), 923–934 (1989).
9. R. K. Kapania and S. Raciti, "Recent advances in analysis of laminated beams and plates, part II: vibrations and wave propagation," *AIAA Journal* **27**(7), 935–946 (1989).
10. A. K. Noor and W. S. Burton, "Assessment of shear deformation theories for multilayered composite plates," *Applied Mechanics Review* **42**(1), 1–13 (1989).
11. E. Reissner and Y. Stavsky, "Bending and stretching of certain types of heterogeneous aelotropic elastic plates," *Journal of Applied Mechanics, Transactions ASME* **28**, 402–408 (1961).
12. S. A. Ambartsumyan, *Theory of Anisotropic Plates*, Technomic, Stanford, CT, 1970.
13. J. M. Whitney and A. W. Leissa, "Analysis of heterogeneous anisotropic plates," *Journal of Applied Mechanics, Transactions ASME* **36**(2), 261–266 (1969).

14. J. N. Reddy, *Energy and Variational Methods in Applied Mechanics*, John Wiley, New York, 1984.
15. J. M. Whitney, *Structural Analysis of Laminated Anisotropic Plates*, Technomic, Lancaster, PA, 1987.
16. A. B. Basset, "On the extension and flexure of cylindrical and spherical thin elastic shells," *Philosophical Transactions of the Royal Society* (London) Ser. A, **181**(6), 433–480 (1980).
17. E. Reissner, "On the theory of bending of elastic plates," *Journal of Mathematics and Physics* **23**(4), 184–191 (1944).
18. E. Reissner, "The effect of transverse shear deformation on the bending of elastic plates," *Journal of Applied Mechanics ASME* **12**, 69–77 (1945).
19. E. Reissner, "On bending of elastic plates," *Quarterly Journal of Applied Mathematics* **5**(1), 55–68 (1947).
20. H. Hencky, "Uber die berucksichtigung der schubverzerrung in ebenen platten," *Ingénieur-Archiv* **16**, 72–766 (1947).
21. F. B. Hildebrand, E. Reissner and G. B. Thomas, "Notes on the foundations of the theory of small displacements of orthotropic shells," NASA TN-1833, Washington, DC (1949).
22. R. D. Mindlin, "Influence of rotatory inertia and shear on flexural motions of isotropic, elastic plates," *Journal of Applied Mechanics, Transactions ASME* **18**, 31–38 (1951).
23. E. A. Reissner, "A consistent treatment of transverse shear deformations in laminated anisotropic plates," *AIAA Journal* **10**(5), 716–718 (1961).
24. J. M. Whitney and C. T. Sun, "A higher order theory for extensional motion of laminated composites," *Journal of Sound and Vibration* **30**(1), 85–97 (1973).
25. G. Jemeilita, "Techniczna teoria plyt s'redniej grubosci" (technical theory of plates with moderate thickness), *Rozprawy inżynierskie (Engineering Transactions), Polska Akademia Nauk* **23**(3), 483–499 (1975).
26. R. Schmidt, "A refined nonlinear theory of plates with transverse shear deformation," *Journal of Industrial Mathematics Society* **27**(1), 23–38 (1977).
27. A. V. Krishna Murty, "Higher order theory for vibration of thick plates," *AIAA Journal* **15**(12), 1823–1824 (1977).
28. K. H. Lo, R. M. Christensen and E. M. Wu, "A high-order theory of plate deformation, part 1: homogeneous plates," *Journal of Applied Mechanics, Transactions ASME* **44**(4), 663–668 (1977).
29. K. H. Lo, R. M. Christensen and E. M. Wu, "A high-order theory of plate deformation, part 2: laminated plates," *Journal of Applied Mechanics, Transactions ASME* **44**(4), 669–676 (1977).
30. M. Levinson, "An accurate, simple theory of the statistics and dynamics of elastic plates," *Mechanical Research Communication* **7**(6), 343–350 (1980).
31. P. Seide, "An improved approximate theory for the bending of laminated plates," *Mechanics Today* **5**, 451–466 (1980).
32. M. V. V. Murthy, "An improved transverse shear deformation theory for laminated anisotropic plates," NASA Tech. Paper, 1903, pp. 1–37, Nov. 1981.
33. L. W. Rehfield and P. L. N. Murthy, "Toward a new engineering theory of bending: fundamentals," *AIAA Journal* **20**(5), 693–699 (1982).
34. L. W. Rehfield and R. R. Valisetty, "A comprehensive theory for planar bending of composite laminates," *Computers and Structures* **15**, 441–447 (1983).
35. J. N. Reddy, "A simple higher-order theory for laminated composite plates," *Journal of Applied Mechanics, Transactions ASME* **51**, 745–752 (1984).
36. J. N. Reddy, "A refined nonlinear theory of plates with transverse shear deformation," *International Journal of Solids and Structures* **20**(9/10), 881–896 (1984).
37. A. Bhimaraddi and L. K. Stevens, "A higher order theory for free vibration of orthotropic, homogeneous, and laminated rectangular plates," *Journal of Applied Mechanics, Transactions ASME* **51**, 195–198 (1984).
38. M. Di Sciuva, "A refined transverse shear deformation theory for multilayered anisotropic plates," *Atti dell' Academia delle Scienze, Torino* **118**, 279–295 (1984).
39. B. F. Vlasov, "Ob uravneniyakh teovii isgiba plastinok (on the equations on the theory of bending of plates)," *Izvestiya Akademie Nauk SSR, OTN* **4**, 102–109 (1958).
40. J. G. Ren, "A new theory of laminated plate," *Computer Science and Technology* **26**(3), 225–239 (1986).
41. S. N. Chatterjee and S. V. Kilharni, "Shear correction factors for laminated plates," *AIAA Journal* **17**(5), 498–499 (1979).
42. J. M. Whitney, "Shear correction factors for orthotropic laminates under static load," *Journal of Applied Mechanics, Transactions ASME* **40**(1), 302–304 (1973).
43. C. W. Bert, "Simplified analysis of static shear factors for beams of nonhomogeneous cross section," *Journal of Composite Materials* **7**, 525–529 (1973).
44. Y. Stavsky, "On the theory of symmetrically heterogeneous plates having the same thickness variation of the elastic moduli," in *Topics in Applied Mechanics*, E. Schwerin Memorial Volume (edited by D. Abir, F. Ollendorff and M. Reiner), pp. 105–166, Elsevier, New York, 1965.
45. P. C. Yang, C. H. Norris and Y. Stavsky, "Elastic wave propagation in heterogeneous plates," *International Journal of Solids and Structures* **2**, 665–684 (1966).
46. J. M. Whitney, "The effects of transverse shear deformation in the bending of laminated plates," *Journal of Composite Materials* **3**, 534–547 (1969).
47. J. M. Whitney and N. J. Pagano, "Shear deformation in heterogeneous anisotropic plates," *Journal of Applied Mechanics, Transactions ASME* **37**(4), 1031–1036 (1970).
48. L. Librescu, *Elastostatics and Kinetics of Anisotropic and Heterogeneous Shell-Type Structures*, Noordhoff, Leyden, Netherlands, 1975.
49. W. Bielski and J. J. Telega, "On existence of solutions for geometrically nonlinear shells and plates," *Zeitschrift für angewandte Mathematik und Mechanik* **68**(4), 155–157 (1988).
50. T. Lewinski, "A note on recent developments in the theory of elastic plates with moderate thickness," *Rozprawy inżynierskie* **34**(4), 531–542 (1986).
51. Z. Rychter, "A sixth-order plate theory-derivation and error estimates," *Journal of Applied Mechanics, Transactions ASME* **54**, 275–279 (1987).
52. J. N. Reddy and W. C. Chao, "A comparison of closed-form and finite element solutions of thick laminated anisotropic rectangular plates," *Nuclear Engineering and Design* **64**, 153–167 (1981).
53. J. N. Reddy, "Simple finite elements with relaxed continuity for nonlinear analysis of plates," Proceedings of 3rd International Conference on Finite Element Methods, Australia, pp. 265–281, July 1979.
54. J. N. Reddy, "A penalty plate-bending element for the analysis of laminated anisotropic composite plates," *International Journal of Numerical Methods in Engineering* **15**, 1187–1206 (1980).
55. J. N. Reddy, "Analysis of layered composite plates accounting for large deflections and transverse shear strains," in *Recent Advances in Nonlinear Computational Mechanics* (edited by E. Hinton, D. R. J. Owen and C. Taylor), pp. 155–202, 1982.
56. J. N. Reddy, "Geometrically nonlinear transient analysis of laminated composite plates," *AIAA Journal* **21**(4), 621–629 (1983).
57. J. N. Reddy, "On refined computational models of composite laminates," *International Journal of Numerical Methods in Engineering* **27**, 361–382 (1989).

58. T. Kant, "Numerical analysis of thick plates," *Computer Methods in Applied Mechanics and Engineering* **31**(1), 1–18 (1982).
59. T. Kant and B. N. Pandya, "A simple finite element formulation of a higher-order theory for unsymmetrically laminated composite plates," *Computers and Structures* **9**, 215–246 (1988).
60. T. Kant and Mallikarjuna, "A higher-order theory for the vibration of unsymmetrically laminated composite and sandwich plates—finite element evaluations," *Computers and Structures* **32**, 1125–1132 (1989).
61. P. N. Pandya and T. Kant, "A refined higher-order generally orthotropic C^0 plate bending element," *Computers and Structures* **28**, 119–133 (1988).
62. J. J. Engblom and O. O. Ochoa, "Finite element formulation including interlaminar stress calculations," *Computers and Structures* **23**, 241–249 (1986).
63. N. D. Phan and J. N. Reddy, "Analysis of laminated composite plates using a higher-order shear deformation theory," *International Journal of Numerical Methods in Engineering* **12**, 2201–2219 (1985).
64. J. G. Ren and E. Hinton, "The finite element analysis of homogeneous and laminated composite plates using a simple higher order theory," *Comm. Applied Numerical Methods* **2**(2), 217–228 (1986).
65. J. G. Ren, "Bending of simply-supported, antisymmetrically laminated rectangular plate under transverse loading," *Computers in Science and Technology* **28**(3), 231–243 (1987).
66. N. S. Putcha and J. N. Reddy, "A mixed finite element for the analysis of laminated plates," in *Advances in Aerospace Structures, Materials and Dynamics* (edited by U. Yuceoglu *et al.*), ASME AD-06, pp. 31–39, 1983.
67. N. S. Putcha and J. N. Reddy, "A refined mixed shear flexible finite element for the nonlinear analysis of laminated plates," *Computers and Structures* **22**, 529–538 (1986).
68. N. S. Putcha and J. N. Reddy, "Stability and natural vibration analysis of laminated plates by using a mixed element based on a refined plate theory," *Journal of Sound and Vibration* **104**(2), 285–300 (1986).
69. J. N. Reddy, "On mixed finite-element formulations of a higher-order theory of composite laminates," *Finite Element Methods for Plate and Shell Structures* (edited by T. J. R. Hughes and E. Hinton), pp. 31–57, Pineridge Press, U.K., 1986.
70. J. L. Doong, "Vibration and stability of an initially stressed thick plate according to a high-order deformation theory," *Journal of Sound and Vibration* **113**(3), 425–440 (1987).
71. O. C. Zienkiewciz, R. L. Taylor and J. M. Too, "Reduced integration technique in general analysis of plates and shells," *International Journal of Numerical Methods in Engineering* **3**, 275–290 (1971).
72. S. F. Pawsey and R. W. Clough, "Improved numerical integration of thick shell finite elements," *International Journal of Numerical Methods in Engineering* **3**, 575–586 (1971).
73. T. J. R. Hughes, M. Cohen and M. Haroun, "Reduced and selective integration techniques in the finite element analysis of plates," *Nuclear Engineering and Design* **46**, 203–222 (1978).
74. D. S. Malkus and T. J. R. Hughes, "Mixed finite element methods—reduced and selective integration techniques: a unification of concepts," *Computing Methods in Applied Mechanics and Engineering* **15**, 63–81 (1978).
75. S. W. Lee and T. H. H. Pian, "Improvement of plate and shell finite elements by mixed formulations," *AIAA Journal* **16**, 29–34 (1978).
76. R. L. Spilker and N. I. Munir, "The hybrid-stress model for thin plates," *International Journal of Numerical Methods in Engineering* **15**, 1239–1260 (1980).
77. K. C. Park and G. M. Stanley, "A curved C^0 shell element based on assumed natural-coordinate strains," *Journal of Applied Mechanics* **53**, 278–290 (1986).
78. K. J. Bathe, E. N. Dvorkin and L. W. Ho, "Our discrete-kirchhoff and isoparametric shell elements for nonlinear analysis—an assessment," *Computers and Structures* **16**, 89–98 (1983).
79. O. C. Zienkiewicz and E. Hinton, "Reduced integration, function smoothing and non-conformity in finite element analysis (with special reference to thick plates)," *Journal of Franklin Institute* **302**(5/6), 443–461 (1976).
80. E. D. L. Pugh, E. Hinton and O. C. Zienkiewicz, "A study of quadrilateral plate bending elements with 'reduced' integration," *International Journal of Numerical Methods in Engineering* **12**, 1059–1079 (1978).
81. G. Prathap and G. R. Bhashyam, "Reduced integration and the shear-flexible beam element," *International Journal of Numerical Methods in Engineering* **18**, 195–210 (1982).
82. R. J. Melosh, "Basis for derivation of matrices for the direct stiffness method," *AIAA Journal* **1**, 1631–1637 (1963).
83. R. C. Averill, "On the behavior of shear deformable plate elements," M.Sc. Thesis, Virginia Polytechnic Institute and State University, Blacksburg, VA, 1989.
84. T. J. R. Hughes and M. Cohen, "The heterosis finite element for plate bending," *Computers and Structures*, **9**, 445–450 (1978).
85. IBM FORTRAN Version 2 Interactive Debug Guide and Reference, Document No. SC26-4223-2, Release 3, 1988.